Journal of Applied Mechanics Vol.8, pp.233-242 (August 2005) JSCE

A Relationship between Stabilized FEM and Bubble Function Element Stabilization Method with Orthogonal Basis for Incompressible Flows

Junichi MATSUMOTO*

*Research Scientist, AMRI, National Institute of Advanced Industrial Science and Technology (AIST)
(1-2-1 Namiki Tsukuba, Ibaraki 305-8564), and PRESTO, Japan Science and Technology Agency (JST)

In this paper, a relationship between the stabilized finite element method and the bubble function element stabilization method with orthogonal basis is shown for the unsteady and steady Navier-Stokes equations. A two-level three-level formulation with bubble function, a bubble function element stabilization method, is proposed for incompressible viscous flow. The special bubble function with two-level partition is extended as an orthogonal basis bubble function element. The three-level bubble function is applied to derive a stabilized operator control term. The two-level three-level formulation with the bubble function formulation possesses better stability than the Bubnov-Galerkin formulation with the bubble function.

Key Words : *Navier-Stokes equations, bubble function element stabilization method, two-level three-level finite element approximation, orthogonal basis bubble function element*

1. Introduction

It has recently been found the relationship[1)2)3)] between the stabilized finite element method[4)5)6)] and the bubble function element[7)] in the finite element method. In the steady advection diffusion problem, the bubble function element is equivalent to the streamline-upwind/Petrov-Galerkin (SUPG) finite element method with the P1 element. Some researchers have developed advanced bubble function elements for incompressible fluid flow[8)9)10)11)]. The advanced bubble function elements are established using the bubble function with a scaling parameter according to the cell Peclet number to attain optimal numerical diffusion. The authors[12)13)] have applied this approach to incompressible viscous flow problem using the bubble function element with a stabilized operator control term.

A relationship between the stabilized finite element method and the bubble function element stabilization method is shown for the unsteady and steady problems in this research. A two-level[14)] three-level[13)15)16)] formulation with bubble functions, that is, a bubble function element stabilization method[13)] is proposed for the incompressible Navier-Stokes equations. For the purpose of improvement in stability and accuracy of the calculation, spatial discretization is applied to the mixed interpolations for the velocity and pressure fields by the bubble function element and linear element, respectively. The advanced bubble function formulation, based on the two-level three-level finite element approximation, obtains better stability than the classical bubble function formulation based on the Bubnov-Galerkin approximation[7)].

In the two-level three-level finite element approximation, the bubble function that orthogonally intersects the basis functions of bubble function element is adopted as a two-level bubble function. The stabilized operator control term is derived from the three-level bubble function. To improve the efficiency of the calculation, an effective Fractional Step method with implicit time integration is applied to the discretization[17)18)]. The second order accuracy Adams-Bashforth formulas are used as the linear approximation of advection velocity. The second order linear time integrator is employed to discretize the quasi-linear form in time. As for the numerical examples, the standing vortex problem and lid-driven cavity flow are investigated with respect to the numerical accuracy and stability of bubble function element stabilization method.

2. Basic Equations

The basic equations that govern incompressible viscous flow are written as the following Navier-Stokes equations and the continuity equation in nondimensional form.

$$\dot{\boldsymbol{u}}+\boldsymbol{u}\cdot\nabla\boldsymbol{u}+\text{grad}\, p-\nabla\cdot(\nu\nabla\boldsymbol{u})=\boldsymbol{f} \quad in \quad \Omega\times[0,T], \tag{1}$$

$$\text{div}\ \boldsymbol{u}=0 \quad in \quad \Omega\times[0,T]. \tag{2}$$

$\boldsymbol{u}$, p, ν and $\boldsymbol{f}$ are velocity, pressure, the inverse of the Reynolds number and body force, respectively. Ω is the computational domain of $\mathbf{R}^N$, where $N = 2$ or 3. N is space dimension number. The time interval is denoted $t \in [0,T]$. The boundary conditions are as follows,

$$\boldsymbol{u}=\hat{\boldsymbol{u}} \quad on \quad \Gamma_1, \tag{3}$$

$$(-p\boldsymbol{I}+\nu\nabla\boldsymbol{u})\cdot\boldsymbol{n}=\hat{\boldsymbol{t}} \quad on \quad \Gamma_2, \tag{4}$$

where the Dirichlet and the Neumann boundary conditions are specified on Γ_1 and Γ_2, respectively. In Eqs. (3) and (4), $\hat{\boldsymbol{u}}$ denotes the values given on the boundary, $\boldsymbol{n}$ is the unit outward normal to Γ_2 and $\boldsymbol{I}$ is the identity matrix.

3. Bubble Function Element Stabilization Method

3.1 Mixed Interpolation

The MINI elements used in the spatial discretization of Eqs. (1) and (2) are shown in **Figs. 1** and **2**.

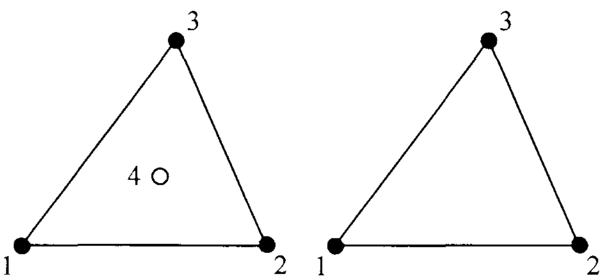

(a) Bubble element (b) Linear element

Fig. 1 Two-dimensional interpolation function.

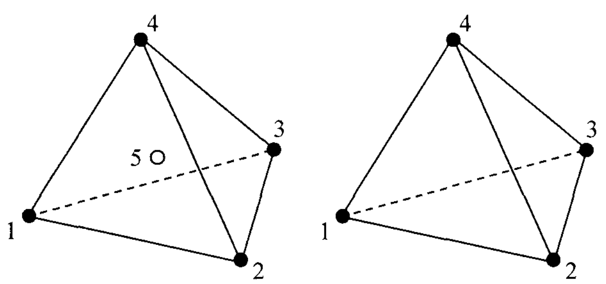

(a) Bubble element (b) Linear element

Fig. 2 Three-dimensional interpolation function.

The mixed interpolations for velocity and pressure are expressed as follows[7].

$$\boldsymbol{u}_h|_{\Omega_e}=\sum_{\alpha=1}^{N+1}\Phi_\alpha\boldsymbol{u}_\alpha+\phi_B\boldsymbol{u}_B, \tag{5}$$

$$p_h|_{\Omega_e}=\sum_{\alpha=1}^{N+1}\Psi_\alpha p_\alpha, \tag{6}$$

$$\Phi_\alpha=\Psi_\alpha-\frac{1}{N+1}\phi_B\ ,\ \alpha=1\cdots N+1. \tag{7}$$

Ω_e is the domain of the element e. Ψ_α are the following shape functions of the linear elements:

Two-dimensional:

$$\Psi_1=1-r-s,\ \Psi_2=r,\ \Psi_3=s, \tag{8}$$

Three-dimensional:

$$\Psi_1=1-r-s-t,\ \Psi_2=r,\ \Psi_3=s,\ \Psi_4=t. \tag{9}$$

Eq. (5) is separated into the linear and bubble function interpolations as follows.

$$\boldsymbol{u}_h|_{\Omega_e}=\bar{\boldsymbol{u}}_h|_{\Omega_e}+\boldsymbol{u}_h^{'}|_{\Omega_e}, \tag{10}$$

$$\bar{\boldsymbol{u}}_h|_{\Omega_e}=\sum_{\alpha=1}^{N+1}\Psi_\alpha\boldsymbol{u}_\alpha, \tag{11}$$

$$\boldsymbol{u}_h^{'}|_{\Omega_e}=\phi_B\boldsymbol{u}_B^{'}, \tag{12}$$

$$\boldsymbol{u}_B^{'}=\boldsymbol{u}_B-\frac{1}{N+1}\sum_{\alpha=1}^{N+1}\boldsymbol{u}_\alpha. \tag{13}$$

3.2 The ξth-Power Bubble Function

The ξth-power bubble functions are defined using isoparametric coordinates $\{r,s\}$ and $\{r,s,t\}$ as shown in **Fig. 3**. The three triangles w_1-w_3 and the four tetrahedra w_1-w_4 are divided at the barycenter. The ξth-power bubble functions of C^0 continuous can be considered for each subtriangle and each tetrahedron as shown in the following equations.

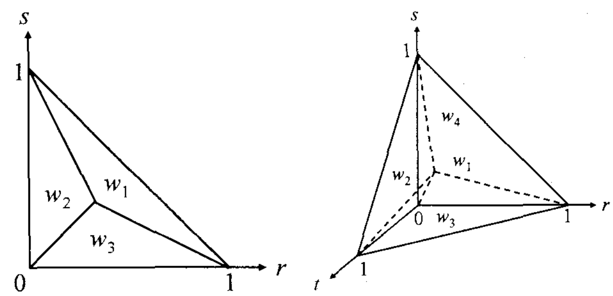

(a) Two dimensions (b) Three dimensions

Fig. 3 The ξth-power bubble function.

Two-dimensional:

$$\phi_B^\xi=\begin{cases}3^\xi\ (1-r-s)^\xi & in\ w_1\\ 3^\xi\ r^\xi & in\ w_2\\ 3^\xi\ s^\xi & in\ w_3\end{cases}\ ,\ (0.0<\xi<\infty), \tag{14}$$

Three-dimensional:

$$\phi_B^\xi=\begin{cases}4^\xi\ (1-r-s-t)^\xi & in\ w_1\\ 4^\xi\ r^\xi & in\ w_2\\ 4^\xi\ s^\xi & in\ w_3\\ 4^\xi\ t^\xi & in\ w_4\end{cases}\ ,\ (0.0<\xi<\infty). \tag{15}$$

The bubble functions have the following property.

$$\langle \Psi_\alpha, \phi_B^\xi \rangle_{\Omega_e} = \frac{1}{N+1} \langle 1, \phi_B^\xi \rangle_{\Omega_e}, \quad \alpha = 1 \cdots N+1. \tag{16}$$

$\langle \cdot \ , \ \cdot \rangle_{\Omega_e}$ denotes the L_2-inner product restricted to Ω_e.

3.3 Two-Level Three-Level Finite Element Approximation

The two-level three-level finite element approximation [13] is considered to be a variation of the problem of finite element space with the bubble function element. In the two-level three-level finite element approximation, the two-level partition with a two-level bubble function is employed for the finite element solution and the three-level partition with a three-level bubble function is employed for the weighting function. The piecewise linear finite element space $\bar{\boldsymbol{V}}_h$, Q_h and the bubble function space $\boldsymbol{V}_h^{'}$, $\hat{\boldsymbol{V}}_h^{'}$ are defined by:

$$\bar{\boldsymbol{V}}_h = \{ \bar{\boldsymbol{v}}_h \in (H_0^1(\Omega))^N ; \ \bar{\boldsymbol{v}}_h|_{\Omega_e} \in (P1(\Omega_e))^N \}, \tag{17}$$

$$\boldsymbol{V}_h^{'} = \{ \boldsymbol{v}_h^{'} \in (H_0^1(\Omega))^N ; \ \boldsymbol{v}_h^{'}|_{\Omega_e} = \phi_B \boldsymbol{v}_B^{'}, \ \boldsymbol{v}_B^{'} \in \mathbf{R}^N \}, \tag{18}$$

$$\hat{\boldsymbol{V}}_h^{'} = \{ \hat{\boldsymbol{v}}_h^{'} \in (H_0^1(\Omega))^N ; \ \hat{\boldsymbol{v}}_h^{'}|_{\Omega_e} = \varphi_B \boldsymbol{v}_B^{'}, \ \boldsymbol{v}_B^{'} \in \mathbf{R}^N \}, \tag{19}$$

$$Q_h = \{ q_h \in H_0^1(\Omega) ; \ q_h|_{\Omega_e} \in P1(\Omega_e), \ \int_\Omega q_h d\Omega = 0 \}, \tag{20}$$

where ϕ_B and φ_B are the two-level bubble and three-level bubble functions with compact support. The approximation is obtained by calculating the finite element solution $(\boldsymbol{u}_h, p_h) \in \boldsymbol{V}_h \times Q_h$, which is determined by the finite element space of $\boldsymbol{V}_h = \bar{\boldsymbol{V}}_h \oplus \boldsymbol{V}_h^{'}$ for the velocity field and Q_h for the pressure field,

$$\langle \dot{\boldsymbol{u}}_h + \mathcal{L}(\boldsymbol{u}_h)\boldsymbol{u}_h + \text{grad } p_h - \boldsymbol{f}, \hat{\boldsymbol{v}}_h \rangle = 0 \quad \forall \hat{\boldsymbol{v}}_h \in \hat{\boldsymbol{V}}_h, \tag{21}$$

$$\langle \text{div } \boldsymbol{u}_h, q_h \rangle = 0 \quad \forall q_h \in Q_h, \tag{22}$$

where

$$\mathcal{L}(\boldsymbol{u}_h) := \boldsymbol{u}_h \cdot \nabla - \nabla \cdot (\nu \nabla),$$

$$\langle u, v \rangle := \sum_{e=1}^{N_e} \langle u, v \rangle_{\Omega_e} := \sum_{e=1}^{N_e} \int_{\Omega_e} u \ v \ d\Omega.$$

N_e is the number of elements. The finite element solution $\boldsymbol{u}_h$ that belongs to $\boldsymbol{V}_h$ and the weighting function $\hat{\boldsymbol{v}}_h$ that belongs to

$$\hat{\boldsymbol{V}}_h = \bar{\boldsymbol{V}}_h \oplus \{ \boldsymbol{v}_h^{'} + \hat{\boldsymbol{v}}_h^{'} ; \ \boldsymbol{v}_h^{'}|_{\Omega_e} + \hat{\boldsymbol{v}}_h^{'}|_{\Omega_e} = (\phi_B + \varphi_B)\boldsymbol{v}_B^{'} \},$$

can be expressed as follows.

$$\boldsymbol{u}_h = \bar{\boldsymbol{u}}_h + \boldsymbol{u}_h^{'}, \ \hat{\boldsymbol{v}}_h = \bar{\boldsymbol{v}}_h + \boldsymbol{v}_h^{'} + \hat{\boldsymbol{v}}_h^{'} = \boldsymbol{v}_h + \hat{\boldsymbol{v}}_h^{'}, \tag{23}$$

where

$$\bar{\boldsymbol{u}}_h, \ \bar{\boldsymbol{v}}_h \in \bar{\boldsymbol{V}}_h, \ \boldsymbol{u}_h^{'} = \sum_{e=1}^{N_e} \phi_B \boldsymbol{u}_B^{'} \in \boldsymbol{V}_h^{'},$$

$$\boldsymbol{v}_h^{'} = \sum_{e=1}^{N_e} \phi_B \boldsymbol{v}_B^{'} \in \boldsymbol{V}_h^{'}, \ \hat{\boldsymbol{v}}_h^{'} = \sum_{e=1}^{N_e} \varphi_B \boldsymbol{v}_B^{'} \in \hat{\boldsymbol{V}}_h^{'}. \tag{24}$$

In the approximation, the two-level bubble and three-level bubble functions are defined elementwise. Finite element equations (21) and (22) that are applied to the bubble function element stabilization method can be written as follows,

$$\langle \dot{\boldsymbol{u}}_h + \mathcal{L}(\boldsymbol{u}_h)\boldsymbol{u}_h + \text{grad } p_h - \boldsymbol{f}, \boldsymbol{v}_h \rangle + \sum_{e=1}^{N_e} \nu^{'} \|\nabla \phi_B\|_{\Omega_e}^2 \boldsymbol{u}_B^{'} \boldsymbol{v}_B^{'} = 0 \quad \forall \boldsymbol{v}_h \in \boldsymbol{V}_h, \tag{25}$$

$$\langle \text{div } \boldsymbol{u}_h, q_h \rangle = 0 \quad \forall q_h \in Q_h, \tag{26}$$

where

$$\nu^{'} \|\nabla \phi_B\|_{\Omega_e}^2 \boldsymbol{u}_B^{'} := \langle \dot{\boldsymbol{u}}_h + \mathcal{L}(\boldsymbol{u}_h)\boldsymbol{u}_h + \text{grad } p_h - \boldsymbol{f}, \varphi_B \rangle_{\Omega_e}, \tag{27}$$

$$\|u\|_{\Omega_e}^2 := \langle u, u \rangle_{\Omega_e}.$$

$\nu^{'}$ $(-\infty < \nu^{'} < \infty)$ and $\nu^{'} \|\nabla \phi_B\|_{\Omega_e}^2 \boldsymbol{u}_B^{'}$ are the stabilized operator control parameter and the stabilized operator control term[13] for the bubble function element.

3.4 Relationship with the Stabilized Finite Element Method

(1) The Unsteady Problem

Finite element equations (25) and (26) that employ the θ method for temporal discretization are described as follows,

$$\langle \frac{\Delta \boldsymbol{u}_h^{n+1}}{\Delta t} + \theta \mathcal{L}(\bar{\boldsymbol{u}}_h^*) \Delta \boldsymbol{u}_h^{n+1} + \mathcal{L}(\bar{\boldsymbol{u}}_h^*) \boldsymbol{u}_h^n + \vartheta \text{grad } \Delta p_h^{n+1} + \text{grad } p_h^n - \boldsymbol{f}, \boldsymbol{v}_h \rangle + \sum_{e=1}^{N_e} \nu^{'} \|\nabla \phi_B\|_{\Omega_e}^2 \{ \theta \Delta \boldsymbol{u}_B^{'n+1} + \boldsymbol{u}_B^{'n} \} \boldsymbol{v}_B^{'} = 0 \quad \forall \boldsymbol{v}_h \in \boldsymbol{V}_h, \tag{28}$$

$$\langle \vartheta \text{div } \Delta \boldsymbol{u}_h^{n+1} + \text{div } \boldsymbol{u}_h^n, q_h \rangle = 0 \quad \forall q_h \in Q_h, \tag{29}$$

where

$$\bar{\boldsymbol{u}}_h^* := \theta^* \bar{\boldsymbol{u}}_h^{n-1} + (1-\theta^*) \bar{\boldsymbol{u}}_h^n, \ \Delta \boldsymbol{u}_h^{n+1} := \boldsymbol{u}_h^{n+1} - \boldsymbol{u}_h^n,$$

$$\Delta \boldsymbol{u}_B^{'n+1} := \boldsymbol{u}_B^{'n+1} - \boldsymbol{u}_B^{'n}, \ \Delta p_h^{n+1} := p_h^{n+1} - p_h^n,$$

$$0 \le \theta \le 1, \ -1 \le \theta^* \le 0, \ 0 \le \vartheta \le 1.$$

Δt is the time increment. $\bar{\boldsymbol{u}}_h^*$ is a constant value defined elementwise by means of the linear finite element solution $\bar{\boldsymbol{u}}_h$. To eliminate $\boldsymbol{u}_B^{'}$ by static condensation, the following two equations are derived according to Eq. (28).

$$\langle \frac{\Delta \boldsymbol{u}_h^{n+1}}{\Delta t} + \theta \mathcal{L}(\bar{\boldsymbol{u}}_h^*) \Delta \boldsymbol{u}_h^{n+1} + \mathcal{L}(\bar{\boldsymbol{u}}_h^*) \boldsymbol{u}_h^n + \vartheta \text{grad } \Delta p_h^{n+1} + \text{grad } p_h^n - \boldsymbol{f}, \bar{\boldsymbol{v}}_h \rangle = 0, \tag{30}$$

$$\langle\frac{\Delta \boldsymbol{u}_h^{n+1}}{\Delta t} + \theta\mathcal{L}(\bar{\boldsymbol{u}}_h^*)\Delta\boldsymbol{u}_h^{n+1} + \mathcal{L}(\bar{\boldsymbol{u}}_h^*)\boldsymbol{u}_h^n + \vartheta \text{grad } \Delta p_h^{n+1} + \text{grad } p_h^n - \boldsymbol{f}, \phi_B\rangle_{\Omega_e} + \nu' \|\nabla\phi_B\|_{\Omega_e}^2 \{\theta\Delta\boldsymbol{u}_B^{'n+1} + \boldsymbol{u}_B^{'n}\} = 0. \quad (31)$$

According to Eq. (31), $\boldsymbol{u}_B^{'n}$ can be expressed as

$$\boldsymbol{u}_B^{'n} = -\tau_{eB}[\langle\frac{\Delta\bar{\boldsymbol{u}}_h^{n+1}}{\Delta t} + \theta\mathcal{L}(\bar{\boldsymbol{u}}_h^*)\Delta\bar{\boldsymbol{u}}_h^{n+1} + \mathcal{L}(\bar{\boldsymbol{u}}_h^*)\bar{\boldsymbol{u}}_h^n + \vartheta\text{grad } \Delta p_h^{n+1} + \text{grad } p_h^n - \boldsymbol{f}, \phi_B\rangle_{\Omega_e} + \{\langle\frac{\phi_B}{\Delta t} + \theta\mathcal{L}(\bar{\boldsymbol{u}}_h^*)\phi_B, \phi_B\rangle_{\Omega_e} + \theta\nu'\|\nabla\phi_B\|_{\Omega_e}^2\}\Delta\boldsymbol{u}_B^{'n+1}]\frac{A_e}{\langle\phi_B, 1\rangle_{\Omega_e}^2}, \quad (32)$$

where

$$\tau_{eB} := \{\langle\mathcal{L}(\bar{\boldsymbol{u}}_h^*)\phi_B, \phi_B\rangle_{\Omega_e} + \nu'\|\nabla\phi_B\|_{\Omega_e}^2\}^{-1}\frac{\langle\phi_B, 1\rangle_{\Omega_e}^2}{A_e}, \quad (33)$$

$$A_e := \int_{\Omega_e} d\Omega.$$

Substituting Eq. (32) for Eqs. (30) and (29), the problem of solving finite element equations (30) and (29) is regarded as the problem that finds the element solution $(\boldsymbol{u}_h^{n+1}, p_h^{n+1}) \in \boldsymbol{V}_h \times Q_h$.

$$\langle\frac{\Delta\bar{\boldsymbol{u}}_h^{n+1}}{\Delta t} + \theta\mathcal{L}(\bar{\boldsymbol{u}}_h^*)\Delta\bar{\boldsymbol{u}}_h^{n+1} + \mathcal{L}(\bar{\boldsymbol{u}}_h^*)\bar{\boldsymbol{u}}_h^n + \vartheta\text{grad } \Delta p_h^{n+1} + \text{grad } p_h^n - \boldsymbol{f}, \bar{\boldsymbol{v}}_h\rangle + \sum_{e=1}^{N_e}\langle\frac{\phi_B}{\Delta t} + \theta\mathcal{L}(\bar{\boldsymbol{u}}_h^*)\phi_B, \bar{\boldsymbol{v}}_h\rangle_{\Omega_e}\Delta\boldsymbol{u}_B^{'n+1}$$
$$- \sum_{e=1}^{N_e}\langle\mathcal{L}(\bar{\boldsymbol{u}}_h^*)\phi_B, \bar{\boldsymbol{v}}_h\rangle_{\Omega_e}\tau_{eB}\langle\frac{\Delta\bar{\boldsymbol{u}}_h^{n+1}}{\Delta t} + \theta\mathcal{L}(\bar{\boldsymbol{u}}_h^*)\Delta\bar{\boldsymbol{u}}_h^{n+1} + \mathcal{L}(\bar{\boldsymbol{u}}_h^*)\bar{\boldsymbol{u}}_h^n + \vartheta\text{grad } \Delta p_h^{n+1} + \text{grad } p_h^n - \boldsymbol{f}, \phi_B\rangle_{\Omega_e}\frac{A_e}{\langle\phi_B, 1\rangle_{\Omega_e}^2}$$
$$- \sum_{e=1}^{N_e}\langle\mathcal{L}(\bar{\boldsymbol{u}}_h^*)\phi_B, \bar{\boldsymbol{v}}_h\rangle_{\Omega_e}\tau_{eB}\{\langle\frac{\phi_B}{\Delta t} + \theta\mathcal{L}(\bar{\boldsymbol{u}}_h^*)\phi_B, \phi_B\rangle_{\Omega_e} + \theta\nu'\|\nabla\phi_B\|_{\Omega_e}^2\}\Delta\boldsymbol{u}_B^{'n+1}\frac{A_e}{\langle\phi_B, 1\rangle_{\Omega_e}^2} = 0 \quad \forall\boldsymbol{v}_h \in \boldsymbol{V}_h, \quad (34)$$

$$\langle\vartheta\text{div } \Delta\bar{\boldsymbol{u}}_h^{n+1} + \text{div } \bar{\boldsymbol{u}}_h^n, q_h\rangle + \sum_{e=1}^{N_e}\langle\vartheta\nabla\phi_B, q_h\rangle_{\Omega_e}\Delta\boldsymbol{u}_B^{'n+1}$$
$$- \sum_{e=1}^{N_e}\langle\nabla\phi_B, q_h\rangle_{\Omega_e}\tau_{eB}\langle\frac{\Delta\bar{\boldsymbol{u}}_h^{n+1}}{\Delta t} + \theta\mathcal{L}(\bar{\boldsymbol{u}}_h^*)\Delta\bar{\boldsymbol{u}}_h^{n+1} + \mathcal{L}(\bar{\boldsymbol{u}}_h^*)\bar{\boldsymbol{u}}_h^n + \vartheta\text{grad } \Delta p_h^{n+1} + \text{grad } p_h^n - \boldsymbol{f}, \phi_B\rangle_{\Omega_e}\frac{A_e}{\langle\phi_B, 1\rangle_{\Omega_e}^2}$$
$$- \sum_{e=1}^{N_e}\langle\nabla\phi_B, q_h\rangle_{\Omega_e}\tau_{eB}\{\langle\frac{\phi_B}{\Delta t} + \theta\mathcal{L}(\bar{\boldsymbol{u}}_h^*)\phi_B, \phi_B\rangle_{\Omega_e} + \theta\nu'\|\nabla\phi_B\|_{\Omega_e}^2\}\Delta\boldsymbol{u}_B^{'n+1}\frac{A_e}{\langle\phi_B, 1\rangle_{\Omega_e}^2} = 0 \quad \forall q_h \in Q_h. \quad (35)$$

Eqs. (34) and (35) are regarded as a multiscale (adjoint)-type[19)20)] stabilized finite element aproximation.

(2) The Steady Problem

Let us consider the case of a steady problem,

$$\Delta\bar{\boldsymbol{u}}_h^{n+1} \to 0, \ \bar{\boldsymbol{u}}_h^n \to \bar{\boldsymbol{u}}_h, \ \Delta\boldsymbol{u}_B^{'n+1} \to 0, \ \boldsymbol{u}_B^{'n} \to \boldsymbol{u}_B^{'},$$

$$\Delta p_h^{n+1} \to 0, \ p_h^n \to p_h,$$

and the case of $\phi_B = \phi_B^\xi$ with $\xi > 1(\xi - 1 > 0)$,

$$\phi_B^{\xi-1} = 0 \quad on \quad \Gamma_e, \quad \Omega_e \in \Omega, \quad (36)$$

thus,

$$\langle\phi_{B,i}^\xi, \cdot\rangle_{\Gamma_e} = \langle(\xi\phi_{B,i})\phi_B^{\xi-1}, \cdot\rangle_{\Gamma_e} = 0. \quad (37)$$

Finite element equations (34) and (35) are rewritten as the following equations:

$$\langle\mathcal{L}(\bar{\boldsymbol{u}}_h^*)\bar{\boldsymbol{u}}_h + \text{grad } p_h - \boldsymbol{f}, \bar{\boldsymbol{v}}_h\rangle + \sum_{e=1}^{N_e}\langle\phi_B, \mathcal{L}^*(\bar{\boldsymbol{u}}_h^*)\bar{\boldsymbol{v}}_h\rangle_{\Omega_e}\tau_{eB}\langle\mathcal{L}(\bar{\boldsymbol{u}}_h^*)\bar{\boldsymbol{u}}_h + \text{grad } p_h - \boldsymbol{f}, \phi_B\rangle_{\Omega_e}\frac{A_e}{\langle\phi_B, 1\rangle_{\Omega_e}^2} = 0 \quad \forall\bar{\boldsymbol{v}}_h \in \bar{\boldsymbol{V}}_h, \quad (38)$$

$$\langle\text{div } \bar{\boldsymbol{u}}_h, q_h\rangle + \sum_{e=1}^{N_e}\langle\phi_B, \nabla q_h\rangle_{\Omega_e}\tau_{eB}\langle\mathcal{L}(\bar{\boldsymbol{u}}_h^*)\bar{\boldsymbol{u}}_h + \text{grad } p_h - \boldsymbol{f}, \phi_B\rangle_{\Omega_e}\frac{A_e}{\langle\phi_B, 1\rangle_{\Omega_e}^2} = 0 \quad \forall q_h \in Q_h, \quad (39)$$

where

$$\mathcal{L}^*(\bar{\boldsymbol{u}}_h^*) := \bar{\boldsymbol{u}}_h^* \cdot \nabla + \nabla \cdot (\nu\nabla).$$

Eqs. (38) and (39) are regarded as the problem that finds the finite element solution $(\bar{\boldsymbol{u}}_h, p_h) \in \bar{\boldsymbol{V}}_h \times Q_h$. The bubble function has the following properties.

$$\langle\phi_B, \nabla \cdot (\nu\nabla\bar{\boldsymbol{v}}_h)\rangle_{\Omega_e} = 0, \quad (40)$$

$$\langle\phi_B, \mathcal{L}^*(\bar{\boldsymbol{u}}_h^*)\bar{\boldsymbol{v}}_h\rangle_{\Omega_e} = \langle\phi_B, \mathcal{L}(\bar{\boldsymbol{u}}_h^*)\bar{\boldsymbol{v}}_h\rangle_{\Omega_e}. \quad (41)$$

Hence, Eqs. (38) and (39) can be expressed as follows.

$$\langle\mathcal{L}(\bar{\boldsymbol{u}}_h^*)\bar{\boldsymbol{u}}_h + \text{grad } p_h - \boldsymbol{f}, \bar{\boldsymbol{v}}_h\rangle + \sum_{e=1}^{N_e}\langle\{\mathcal{L}(\bar{\boldsymbol{u}}_h^*)\bar{\boldsymbol{v}}_h\}, \tau_{eB}\{\mathcal{L}(\bar{\boldsymbol{u}}_h^*)\bar{\boldsymbol{u}}_h + \text{grad } p_h - \boldsymbol{f}\}\rangle_{\Omega_e} = 0 \quad \forall\bar{\boldsymbol{v}}_h \in \bar{\boldsymbol{V}}_h, \quad (42)$$

$$\langle\text{div } \bar{\boldsymbol{u}}_h, q_h\rangle + \sum_{e=1}^{N_e}\langle\{\nabla q_h\}, \tau_{eB}\{\mathcal{L}(\bar{\boldsymbol{u}}_h^*)\bar{\boldsymbol{u}}_h + \text{grad } p_h - \boldsymbol{f}\}\rangle_{\Omega_e} = 0 \quad \forall q_h \in Q_h. \quad (43)$$

These approximations are equivalent to those of the SUPG/PSPG method[6)].

3.5 The Finite Element Equations for the Navier-Stokes Equations

Finite element equations (25) and (26) are obtained from the weak form.

$$\langle \dot{\boldsymbol{u}}_h, \boldsymbol{v}_h\rangle + \langle \bar{\boldsymbol{u}}_h^* \cdot \nabla \boldsymbol{u}_h, \boldsymbol{v}_h\rangle - \langle p_h, \text{div } \boldsymbol{v}_h\rangle + \nu\langle \nabla \bar{\boldsymbol{u}}_h, \nabla \boldsymbol{v}_h\rangle$$

$$+\nu\langle \nabla \boldsymbol{u}_h^{'}, \nabla \boldsymbol{v}_h\rangle + \sum_{e=1}^{N_e} \nu^{'} \|\nabla \phi_B\|^2_{\Omega_e} \boldsymbol{u}_B^{'} \boldsymbol{v}_B^{'}$$

$$= \langle \boldsymbol{f}, \boldsymbol{v}_h\rangle + \langle \hat{\boldsymbol{t}}, \boldsymbol{v}_h\rangle_{\Gamma_2} \quad \forall \boldsymbol{v}_h \in \boldsymbol{V}_h, \tag{44}$$

$$\langle \text{div } \boldsymbol{u}_h, q_h\rangle = 0 \quad \forall q_h \in Q_h. \tag{45}$$

The following property is obtained.

$$\langle \nabla \boldsymbol{u}_h^{'}, \nabla \bar{\boldsymbol{v}}_h\rangle = \sum_{e=1}^{N_e} \langle \nabla \boldsymbol{u}_h^{'}, \nabla \bar{\boldsymbol{v}}_h\rangle_{\Omega_e}$$

$$= \sum_{e=1}^{N_e} \{\langle \phi_B, \nabla \bar{\boldsymbol{v}}_h\rangle_{\Gamma_e} - \langle \phi_B, \nabla\cdot(\nabla \bar{\boldsymbol{v}}_h)\rangle_{\Omega_e}\} \boldsymbol{u}_B^{'}$$

$$= \sum_{e=1}^{N_e} \langle \phi_B, \nabla\cdot(\nabla \bar{\boldsymbol{v}}_h)\rangle_{\Omega_e} \boldsymbol{u}_B^{'} = 0. \tag{46}$$

By substituting Eqs. (46) into Eq. (44), finite element equations can be rewritten as follows.

$$\langle \dot{\boldsymbol{u}}_h, \boldsymbol{v}_h\rangle + \langle \bar{\boldsymbol{u}}_h^* \cdot \nabla \boldsymbol{u}_h, \boldsymbol{v}_h\rangle - \langle p_h, \text{div } v_h\rangle + \nu\langle \bar{u}_{i,j}^h, v_{i,j}^h\rangle$$

$$+\sum_{e=1}^{N_e} (\nu + \nu^{'}) \|\nabla \phi_B\|^2_{\Omega_e} \boldsymbol{u}_B^{'} \boldsymbol{v}_B^{'}$$

$$= \langle \boldsymbol{f}, \boldsymbol{v}_h\rangle + \langle \hat{\boldsymbol{t}}, \boldsymbol{v}_h\rangle_{\Gamma_2} \quad \forall \boldsymbol{v}_h \in \boldsymbol{V}_h, \tag{47}$$

$$\langle \text{div } \boldsymbol{u}_h, q_h\rangle = 0 \quad \forall q_h \in Q_h. \tag{48}$$

If $\tau_{eB} = \tau_{eR}$, Eq. (33) can be arranged the following equation:

$$(\nu + \nu^{'}) \|\nabla \phi_B\|^2_{\Omega_e} = \frac{\langle \phi_B, 1\rangle^2_{\Omega_e}}{A_e} \tau_{eR}^{-1}. \tag{49}$$

where

$$\tau_{eR} = \left[\left(\frac{2|\bar{\boldsymbol{u}}_h^*|}{h_e} \right)^2 + \left(\frac{4\nu}{h_e^2} \right)^2 \right]^{-\frac{1}{2}}. \tag{50}$$

h_e is the element length[6].

4. Two-Level Bubble Function for the Orthogonal Basis Bubble Function Element

The two-level bubble function can employ an arbitrary bubble function. In this research, a special bubble function is proposed as a two-level bubble function. The bubble function orthogonally intersects the basis functions of the bubble function element in accordance with expression (5). The effective bubble function element is named the orthogonal basis bubble function element. The conditions under which the basis functions of the bubble function element cut orthogonally must satisfy the following two condition equations (51) and (52).

$$\langle \Phi_\alpha, \phi_B\rangle_{\Omega_e} = \frac{1}{N+1}\langle 1, \phi_B\rangle_{\Omega_e} - \frac{1}{N+1}\|\phi_B\|^2_{\Omega_e} = 0. \tag{51}$$

If $\alpha \neq \beta$, then

$$\langle \Phi_\alpha, \Phi_\beta\rangle_{\Omega_e} = \langle \Psi_\alpha, \Psi_\beta\rangle_{\Omega_e} - \frac{1}{(N+1)^2}\langle 1, \phi_B\rangle_{\Omega_e} = 0. \tag{52}$$

$$\langle \Psi_\alpha, \phi_B\rangle_{\Omega_e} = \frac{1}{N+1}\langle 1, \phi_B\rangle_{\Omega_e}. \tag{53}$$

$$\alpha = 1\cdots N+1 \ , \ \beta = 1\cdots N+1.$$

Eq. (53) is assumed on the derivation of Eqs. (51) and (52). Finally, the following relation Eq. (54) is obtained from Eqs. (51) and (52).

$$\langle \phi_B, 1\rangle_{\Omega_e} = \|\phi_B\|^2_{\Omega_e} = \frac{N+1}{N+2}A_e. \tag{54}$$

We use Eq. (55) as a two-level bubble function that fulfills Eqs. (51) and (52).

$$\phi_B = \frac{\alpha_1\phi_{B1} + \alpha_2\phi_{B2} + \phi_{B3}}{\alpha_1 + \alpha_2 + 1}. \tag{55}$$

By substituting Eq. (55) into Eqs. (51) and (52), Eqs. (56) and (57) are obtained:

$$\beta_1\alpha_1^2 + \beta_2\alpha_2^2 + \beta_3 + \beta_4\alpha_1\alpha_2 + \beta_5\alpha_1 + \beta_6\alpha_2 = 0 \ , \tag{56}$$

$$\alpha_2 = \gamma_1\alpha_1 + \gamma_2 \ , \tag{57}$$

where

$$\beta_1 = \left(\langle \phi_{B1}, 1\rangle_{\Omega_e} - \|\phi_{B1}\|^2_{\Omega_e}\right) A_e^{-1} \ ,$$

$$\beta_2 = \left(\langle \phi_{B2}, 1\rangle_{\Omega_e} - \|\phi_{B2}\|^2_{\Omega_e}\right) A_e^{-1} \ ,$$

$$\beta_3 = \left(\langle \phi_{B3}, 1\rangle_{\Omega_e} - \|\phi_{B3}\|^2_{\Omega_e}\right) A_e^{-1} \ ,$$

$$\beta_4 = \left(\langle \phi_{B2}, 1\rangle_{\Omega_e} + \langle \phi_{B1}, 1\rangle_{\Omega_e} - 2\langle \phi_{B1}, \phi_{B2}\rangle_{\Omega_e}\right) A_e^{-1} \ ,$$

$$\beta_5 = \left(\langle \phi_{B3}, 1\rangle_{\Omega_e} + \langle \phi_{B1}, 1\rangle_{\Omega_e} - 2\langle \phi_{B1}, \phi_{B3}\rangle_{\Omega_e}\right) A_e^{-1} \ ,$$

$$\beta_6 = \left(\langle \phi_{B3}, 1\rangle_{\Omega_e} + \langle \phi_{B2}, 1\rangle_{\Omega_e} - 2\langle \phi_{B2}, \phi_{B3}\rangle_{\Omega_e}\right) A_e^{-1} \ ,$$

$$\gamma_1 = -\frac{\langle \phi_{B1}, 1\rangle_{\Omega_e} A_e^{-1} - \frac{N+1}{N+2}}{\langle \phi_{B2}, 1\rangle_{\Omega_e} A_e^{-1} - \frac{N+1}{N+2}} \ ,$$

$$\gamma_2 = -\frac{\langle \phi_{B3}, 1\rangle_{\Omega_e} A_e^{-1} - \frac{N+1}{N+2}}{\langle \phi_{B2}, 1\rangle_{\Omega_e} A_e^{-1} - \frac{N+1}{N+2}} \ .$$

By substituting Eq. (57) into Eq. (56), Eq. (58) is obtained:

$$a\ \alpha_1^2 + b\ \alpha_1 + c = 0 \ , \tag{58}$$

$$a = \beta_1 + \beta_2\gamma_1^2 + \beta_4\gamma_1 \ , \ b = 2\beta_2\gamma_1\gamma_2 + \beta_4\gamma_2 + \beta_5 + \beta_6\gamma_1 \ ,$$

$$c = \beta_2\gamma_2^2 + \beta_3 + \beta_6\gamma_2 \ .$$

The quadratic formula (59) is acquired because Eq. (58) is a quadratic equation on α_1.

$$\alpha_1 = \frac{-b \pm \sqrt{b^2 - 4ac}}{2a} \ . \tag{59}$$

α_1, α_2 of Eqs. (58) and (57) are calculated by employing the ξth-power bubble functions of Eq. (60).

$$\phi_{B1} = \phi_B^{\xi_1=3} \ , \ \phi_{B2} = \phi_B^{\xi_2=2} \ , \ \phi_{B3} = \phi_B^{\xi_3=6/5}, \tag{60}$$

Two dimensions:

$$\alpha_1 = \frac{-b + \sqrt{b^2 - 4ac}}{2a} = -0.1393869\cdots \ ,$$
$$\alpha_2 = -0.6433844\cdots, \tag{61}$$

Three dimensions:

$$\alpha_1 = \frac{-b + \sqrt{b^2 - 4ac}}{2a} = 0.7333511\cdots \ ,$$
$$\alpha_2 = -1.6387018\cdots. \tag{62}$$

Eq. (55) satisfies Eq. (37) because of $\xi_1 > 1$, $\xi_2 > 1$, and $\xi_3 > 1$. **Fig. 4** shows the two dimensional bubble function shapes of ϕ_B and ϕ_B^2 with the orthogonal basis bubble function element. In the orthogonal basis bubble function element, the concrete shape of the bubble function does not make sense because the relationship in Eq. (54) is important to the orthogonal conditions of the basis functions.

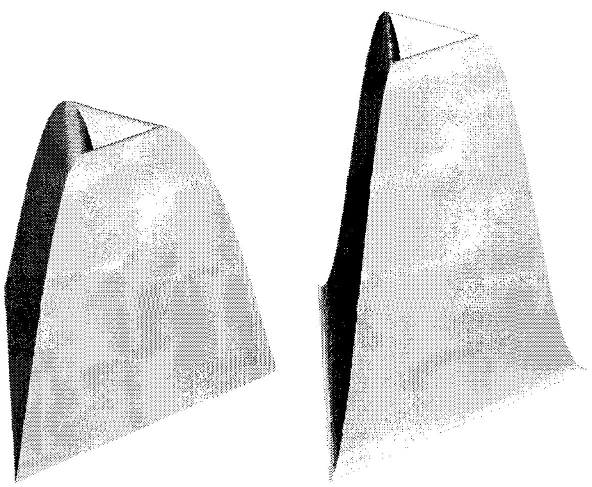

(a) ϕ_B (b) ϕ_B^2

Fig. 4 The bubble function shapes of ϕ_B and ϕ_B^2 with $\langle\phi_B, 1\rangle_{\Omega_e} = \|\phi_B\|^2_{\Omega_e} = \frac{3}{4}A_e$.

5. Three-Level Bubble Function for Stabilized Operator Control Term

The stabilized operator control term is derived from the three-level bubble function. Three-level bubble function assumes that it has the relation of the following equation:

$$\langle\Psi_\alpha, \varphi_B\rangle_{\Omega_e} = \frac{1}{N+1}\langle 1, \varphi_B\rangle_{\Omega_e} \ , \ \alpha = 1\cdots N+1. \tag{63}$$

The following conditions are introduced for the three-level bubble function:

$$\langle 1, \varphi_B\rangle_{\Omega_e} = 0 \ , \tag{64}$$
$$\langle\phi_B, \varphi_B\rangle_{\Omega_e} = 0 \ . \tag{65}$$

By using Eqs. (64) and (65), the right side terms of Eq. (27) are obtained as follows.

$$\langle \dot{\boldsymbol{u}}_h + \mathcal{L}(\boldsymbol{u}_h)\boldsymbol{u}_h + \mathrm{grad}\ p_h - \boldsymbol{f}, \varphi_B\rangle_{\Omega_e} = \nu\langle\nabla\phi_B, \nabla\varphi_B\rangle_{\Omega_e}\boldsymbol{u}_B' \ . \tag{66}$$

We use Eq. (67) as the three-level bubble function that fulfills Eqs. (64) and (65).

$$\varphi_B = \frac{\nu_\varphi}{\nu}\frac{\delta_1\varphi_{B1} + \delta_2\varphi_{B2} + \varphi_{B3}}{\delta_1 + \delta_2 + 1} \ , \ -\infty < \nu_\varphi < \infty, \tag{67}$$

$$\nu' = \frac{\frac{\nu_\varphi}{\delta_1+\delta_2+1}\langle\nabla\phi_B, \nabla\left(\delta_1\varphi_{B1} + \delta_2\varphi_{B2} + \varphi_{B3}\right)\rangle_{\Omega_e}}{\|\nabla\phi_B\|^2_{\Omega_e}} \ . \tag{68}$$

According to Eqs. (67) and (68), the following equation is derived:

$$\nu\langle\nabla\phi_B, \nabla\varphi_B\rangle_{\Omega_e}\boldsymbol{u}_B' = \nu'\|\nabla\phi_B\|^2_{\Omega_e}\boldsymbol{u}_B' \ . \tag{69}$$

By substituting Eq. (67) into Eqs. (64) and (65), Eqs. (70) and (71) are obtaind.

$$\delta_1 = \frac{\langle 1, \varphi_{B2}\rangle_{\Omega_e}\langle\phi_B, \varphi_{B3}\rangle_{\Omega_e} - \langle 1, \varphi_{B3}\rangle_{\Omega_e}\langle\phi_B, \varphi_{B2}\rangle_{\Omega_e}}{\langle 1, \varphi_{B1}\rangle_{\Omega_e}\langle\phi_B, \varphi_{B2}\rangle_{\Omega_e} - \langle 1, \varphi_{B2}\rangle_{\Omega_e}\langle\phi_B, \varphi_{B1}\rangle_{\Omega_e}}, \tag{70}$$

$$\delta_2 = \frac{\langle 1, \varphi_{B3}\rangle_{\Omega_e}\langle\phi_B, \varphi_{B1}\rangle_{\Omega_e} - \langle 1, \varphi_{B1}\rangle_{\Omega_e}\langle\phi_B, \varphi_{B3}\rangle_{\Omega_e}}{\langle 1, \varphi_{B3}\rangle_{\Omega_e}\langle\phi_B, \varphi_{B2}\rangle_{\Omega_e} - \langle 1, \varphi_{B2}\rangle_{\Omega_e}\langle\phi_B, \varphi_{B1}\rangle_{\Omega_e}}. \tag{71}$$

δ_1, δ_2, and ν' of Eqs. (70), (71), and (68) are calculated by employing the ξth-power bubble functions of Eq. (72).

$$\varphi_{B1} = \phi_B^3 \ , \ \varphi_{B2} = \phi_B^2 \ , \ \varphi_{B3} = \phi_B^1 \ , \tag{72}$$

Two dimensions:

$$\delta_1 = 7.4759881\cdots \ , \ \delta_2 = -6.4855929\cdots \ ,$$
$$\nu' = C\ \nu_\varphi \ , \ C = -0.0935697\cdots \ , \tag{73}$$

Three dimensions:

$$\delta_1 = 70.5090640\cdots \ , \ \delta_2 = -37.7545320\cdots \ ,$$
$$\nu' = C\ \nu_\varphi \ , \ C = -0.0338976\cdots \ . \tag{74}$$

Fig. 5 shows the two-dimensional bubble function shapes ($\nu_\varphi = \nu$) of φ_B and $\phi_B\varphi_B$. **Fig. 5** shows the two dimensional bubble function shapes ($\nu_\varphi = \nu$) of φ_B and $\phi_B\varphi_B$. In the three-level bubble function, the concrete shape of the bubble function does not make sense because condition equations (64) and (65) are the key to deriving a stabilized operator control term.

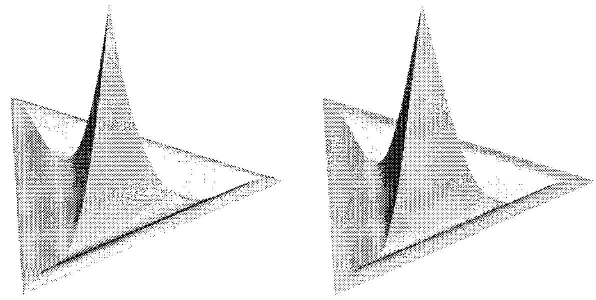

(a) φ_B (b) $\phi_B\varphi_B$

Fig. 5 The bubble function shapes of φ_B and $\phi_B\varphi_B$ with $\langle 1, \varphi_B \rangle_{\Omega_e} = \langle \phi_B, \varphi_B \rangle_{\Omega_e} = 0$.

6. Time Discretization for Finite Element Equations

To discretize finite element equations (47) and (48), a quasi-linear form with $\theta = \frac{1}{2}$, $\theta^* = -\frac{1}{2}$, and $\vartheta = 1$ is givien by

$$\boldsymbol{M}\frac{\boldsymbol{u}_h^{n+1} - \boldsymbol{u}_h^n}{\Delta t} + \boldsymbol{S}(\bar{\boldsymbol{u}}_h^*)\boldsymbol{u}_h^{n+1/2} - \boldsymbol{B}p_h^{n+1} = \boldsymbol{F}, \quad (75)$$

$$\boldsymbol{B}^T\boldsymbol{u}_h^{n+1} = 0, \quad (76)$$

where

$$\bar{\boldsymbol{u}}_h^* = \frac{1}{2}(3\bar{\boldsymbol{u}}_h^n - \bar{\boldsymbol{u}}_h^{n-1}) \ , \ \boldsymbol{u}_h^{n+1/2} = \frac{1}{2}(\boldsymbol{u}_h^{n+1} + \boldsymbol{u}_h^n),$$

are employed. $\boldsymbol{M}$ is the mass matrix, and $\boldsymbol{S}(\bar{\boldsymbol{u}}_h^*)$ is the matrix of the advection term and viscosity term. $\boldsymbol{B}$ is the gradient matrix, and $\boldsymbol{F}$ is the vector of the force term and boundary integration term. The important point to note is that $\boldsymbol{M}$ is the diagonal mass matrix on account of the orthogonal basis bubble function element. To discretize the quasi-linear form in time, a second order linear time integrator is used[17)18)]. To apply the fractional step method, a consistent pressure-poisson equation can be obtained by using an intermediate velocity that does not satisfy Eq. (76). The unknown velocities $\boldsymbol{u}_h^{n+1}$ are replaced with intermediate velocities $\tilde{\boldsymbol{u}}_h^{n+1}$ using the pressure p_h^n. Eq. (75) can thus be expressed as follows.

$$\boldsymbol{M}\frac{\tilde{\boldsymbol{u}}_h^{n+1} - \boldsymbol{u}_h^n}{\Delta t} + \boldsymbol{S}(\bar{\boldsymbol{u}}_h^*)\tilde{\boldsymbol{u}}_h^{n+1/2} - \boldsymbol{B}p_h^n = \boldsymbol{F}, \quad (77)$$

where

$$\tilde{\boldsymbol{u}}_h^{n+1/2} = \frac{1}{2}(\tilde{\boldsymbol{u}}_h^{n+1} + \boldsymbol{u}_h^n).$$

Eq. (78) is obtained by subtracting Eq. (77) from Eq. (75).

$$\boldsymbol{M}\frac{\boldsymbol{u}_h^{n+1} - \tilde{\boldsymbol{u}}_h^{n+1}}{\Delta t} + \frac{1}{2}\boldsymbol{S}(\bar{\boldsymbol{u}}_h^*)\left(\boldsymbol{u}_h^{n+1} - \tilde{\boldsymbol{u}}_h^{n+1}\right) - \boldsymbol{B}\left(p_h^{n+1} - p_h^n\right) = 0. \quad (78)$$

The consistent pressure-poisson equation (79) is derived by multiplying Eq. Eq. (78) by $\boldsymbol{B}^T\boldsymbol{M}^{-1}$ and then substituting Eq. (76) into the resulting equation.

$$\boldsymbol{B}^T\boldsymbol{M}^{-1}\boldsymbol{B}\Delta t\left(p_h^{n+1} - p_h^n\right) = -\boldsymbol{B}^T\tilde{\boldsymbol{u}}_h^{n+1}, \quad (79)$$

where except $\boldsymbol{B}^T\tilde{\boldsymbol{u}}_h^{n+1}$, the left side terms of Eq. (78) are omitted by assuming $(\boldsymbol{u}_h^{n+1} - \tilde{\boldsymbol{u}}_h^{n+1})$ to be an infinitesimal value.

The algorithm of this scheme is written as follows.

1. Start from initial velocity $\boldsymbol{u}_h^{(0)}$ and pressure $p_h^{(0)}$.
2. Compute $\tilde{\boldsymbol{u}}_h^{n+1}$ by Eq. (77).
3. Compute p_h^{n+1} by Eq. (79).
4. Compute $\boldsymbol{u}_h^{n+1}$ by Eq. (78).
5. i = i + 1 go to 2.

Element-by-element BiCGstab method with scaling is used to solve simultaneous equations (77) and (78), and element-by-element CG method with scaling is used to solve simultaneous equation (79).

7. Numerical Examples

7.1 Standing Vortex Problem

To investigate the numerical accuracy of the bubble function element stabilization method, the standing vortex problem is used as numerical example. **Fig. 6** shows the computational domain and initial conditions. The numerical example employs $\Delta t = 0.05$. We compare the results of kinematic energy using the standard bubble function element (classical) and the bubble function element stabilization method (improved). The standard bubble function element means the bubble function element without the stabilized operator control term in Eq. (44). The numerical results are shown in **Fig. 7**. The time history of kinematic energy using the standard bubble function element has a major effect on the result due to divergence. On the other hand, the bubble function element stabilization method conserves kinematic energy with high numerical accuracy.

7.2 Lid-Driven Cavity Flow

To investigate the numerical stability of the bubble function element stabilization method, lid-driven cavity flow is used as a numerical example. **Fig. 8** shows the computational domain, boundary condition, and finite element mesh. Two numerical examples are calculated by using $\Delta t = 0.0001 (Re = 1)$ and $\Delta t = 0.025 (Re = 400)$, respectively. We compare the results of pressure distribution using the standard bubble function element (classical) and bubble function element stabilization method (improved). Numerical results are shown in **Figs. 9** and **10**. The spatial oscillation of pressure using the standard bubble function element has a much great effect on the result. However, the bubble function element stabilization method remedies the oscillation distribution of pressure.

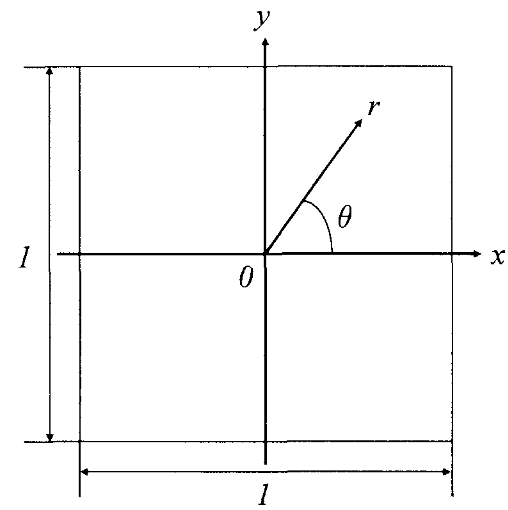

(a) Computational domain

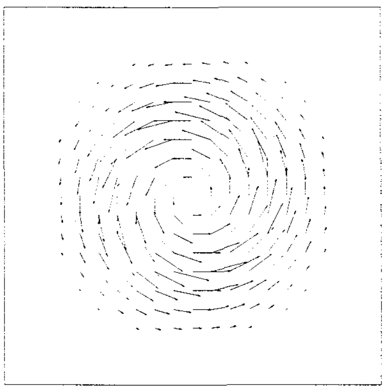

(b) Initial condition

$$u_r = 0, \quad u_\theta = \begin{cases} 5r & r < 0.2 \\ 2 - 5r & 0.2 < r < 0.4 \\ 0 & r > 0.4 \end{cases} . \tag{80}$$

Fig. 6 Standing vortex problem.

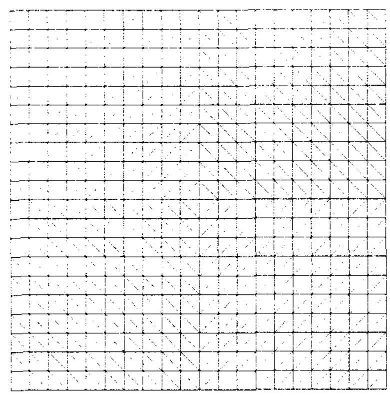

(a) Finite element mesh (20 × 20)

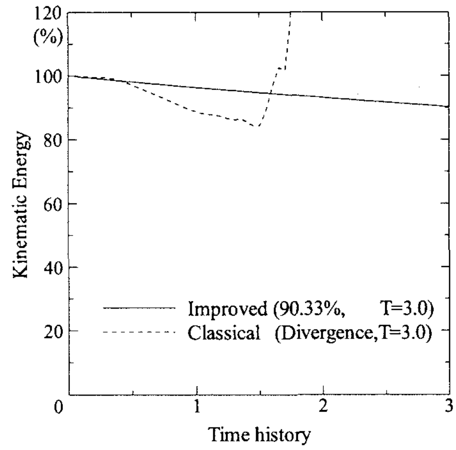

(b) Kinematic energy

Fig. 7 The finite element mesh and the numerical results.

8. Conclusions

The relationship between stabilized finite element method and orthogonal basis bubble function element stabilization method was described for the unsteady and steady Navier-Stokes equations in this paper. The bubble function element stabilization method can be regarded as a multiscale(adjoint)-type stabilized finite element method. The two-level partition with a two-level bubble function was used for the finite element solution and the three-level partition with a three-level bubble function was used for the weighting function. The bubble function that orthogonally intersects the basis functions of the bubble function element was adopted as the two-level bubble function and the stabilized operator control term was derived from the three-level bubble function. The fractional step method for incompressible viscous flow based on bubble function element stabilization method was investigated. The bubble function element stabilization method obtained better numerical accuracy and stability than the classical bubble function method.

REFERENCES

1) Pierre, R.: Simple C^0 approximations for the computation of incompressble flows, *Comput. Methods Appl. Mech. Engrg.* Vol.68, 205-227, 1988.
2) Brezzi, F., Bristeau, M.-O., Franca, L.P., Mallet, M., and Roge, G.: A relationship between stabilized finite element methods and the Galerkin method with bubble functions, *Comput. Methods Appl. Mech. Engrg.* Vol.96, 117-129, 1992.
3) Baicocchi, C., Brezzi, F., and Franca, L.P.: Virtual bubbles and Galerkin-Least-Squares type method(Ga.L.S.), *Comput. Methods Appl. Mech. Engrg.* Vol.105, 125-141, 1993.
4) Brooks, A.N. and Hughes, T.J.R.: Streamline Upwind/Petrov-Galerkin formulations for convection dominated flows with Navier-Stokes equa-

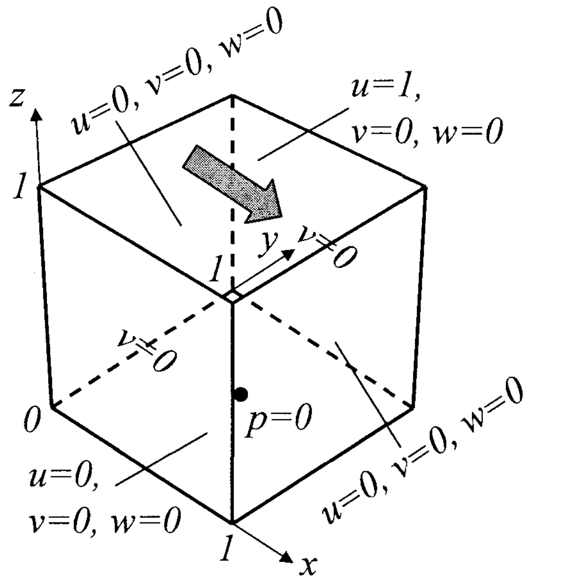

(a) Computational domain and boundary condition

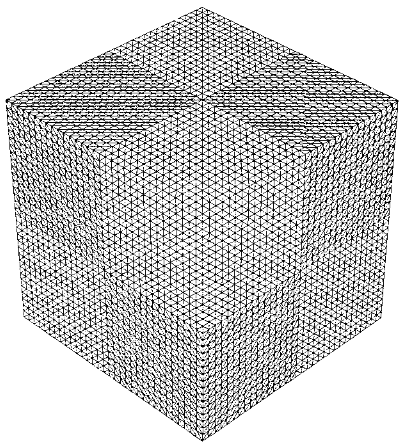

(b) Finite element mesh (32 × 32 × 32)

Fig. 8 Lid-driven cavity flow.

tions, *Comput. Methods Appl. Mech. Engrg.*, Vol.32, pp.199-259, 1982.

5) Hughes, T.J.R., Franca, L.P., and Balestra, M.: A new finite element formulation for computational fluid dynamics: V. Circumventing the Babuska-Brezzi conditon: A stable Petrov-Galerkin formulation of the Stokes problem accommodating equal-order interpolations, *Comput. Methods Appl. Mech. Engrg.*, Vol.59, pp.85-99, 1986.

6) Tezduyar, T.E., Mittal, S., Ray, S.E., and Shih, R.: Incompressible flow computations with stabilized bilinear and linear equal-order-interpolation velocity-pressure element, *Comput. Methods Appl. Mech. Engrg.*, Vol.95, pp.221-242, 1992.

7) Arnold, D.N., Brezzi, F., and Fortin, M.: A Stable Finite Element for the Stokes Equations, *Calcolo*, Vol.23, pp.337-pp.344, 1984.

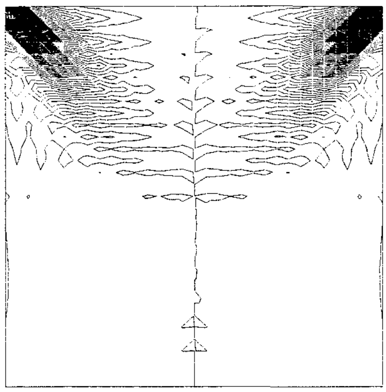

(a) Classical

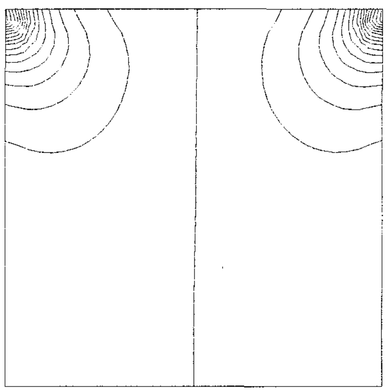

(b) Improved

Fig. 9 Numerical results (Re=1, y=0.5).

8) Simo, J.C., Armero, F., and Taylor, C.A.: Stable and time-dissipative finite element methods for the incompressible Navier-Stokes equations in advection dominated flows, *Int. J. Numer. Meth. Engng.*, Vol.38, pp.1475-1506, 1995.

9) Yamada, T.: A bubble element for the compressible Euler equations, *International Journal of Computational Fluid Dynamics*, Vol.9, pp.273-283, 1998.

10) Brezzi, F., Franca, L.P., and Russo, A.: Further considerations on residual-free bubbles for advective-diffusive equations, *Comput. Methods Appl. Mech. Engrg.*, Vol.166, pp.25-33, 1998.

11) Okumura, H. and Kawahara, M.: A new stable bubble element for incompressible fluid flow based on a mixed Petrov-Galerkin finite element formulation, *International Journal of Computational Fluid Dynamics*, Vol.17(4), pp.275-282, 2003.

12) Matsumoto, J. and Umetsu, T.: A consideration on finite element method analysis of incompressible fluid using bubble function (English translation of the title), *Annual Conference of the Japan Society for Industrial and Applied Mathematics*, pp.46-47, 1996 (Proceedings in Japanese).

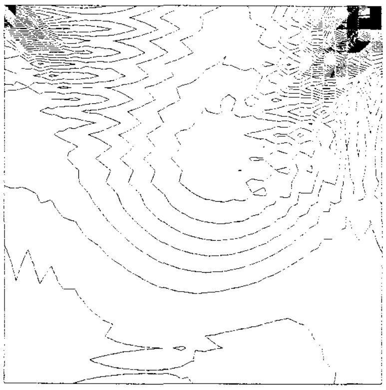

(a) Classical

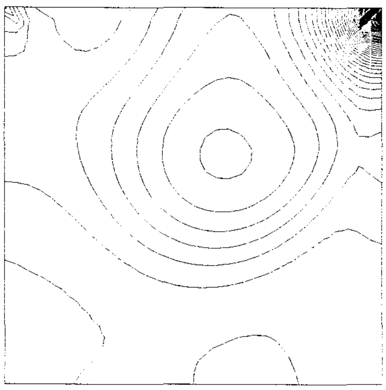

(b) Improved

Fig. 10 Numerical results (Re=400, y=0.5).

13) Matsumoto, J. and Kawahara, M.: Shape identification for fluid-structure interaction problem using improved bubble element, *International Journal of Computational Fluid Dynamics*, Vol.15, pp.33-45, 2001.
14) Hughes, T.J.R., Mazzei, L., Jansen, K.E.: Large Eddy Simulation and the variational multiscale method, *Computing and Visualization in Science*, Vol. 3, pp.47-pp.59, 2000.
15) Collis, S.S.: Monitoring unresolved scales in multiscale turbulence modeling, *Phys. Fluids*, Vol. 13, pp.1800-1806, 2001.
16) Gravemeier, V., Wall, W.A., and Ramm, E.: A three-level finite element method for the instationary incompressible Navier-Stokes equations, *Comput. Methods Appl. Mech. Engrg.*, 193, pp.1323-1366, 2004.
17) Simo, J.C. and Armero, F.: Unconditional stability and long-term behaver of transient algorithms for the incompressible Navier-Stokes and Euler Equations, *Comput. Methods Appl. Mech. Engrg.*, Vol.111, pp.111-154, 1994.
18) Maruoka, A., Matsumoto, J., and Kawahara, M.: A fractional step finite element method for incompressible Navier-Stokes equations using quadrilateral scaled bubble function, *Journal of Structural Engineering* (JSCE), 44A, pp.383-390, 1998 (in Japanese).
19) Hughes, T.J.R., Feijoo, G.R., Mazzei, L., and Quincy, J.-B.: The variational multiscale method–a paradigm for computational mechanics, *Comput. Methods Appl. Mech. Engrg.*, Vol.166, pp.3-24, 1998.
20) Stein, E., and Borst, R., Hughes, T.J.R.: *Encyclopedia of Computational Mechanics*, Wiley, Vol.3 Fluids, 2004.

(Received April 15, 2005)